
Beyond U: Making Diffusion Models Faster & Lighter

Sergio Calvo-Ordoñez*, Jiahao Huang†, Lipei Zhang‡,
Guang Yang†, Carola-Bibiane Schönlieb‡, Angelica I Aviles-Rivero‡

Abstract

Diffusion models are a family of generative models that yield record-breaking performance in tasks such as image synthesis, video generation, and molecule design. Despite their capabilities, their efficiency, especially in the reverse denoising process, remains a challenge due to slow convergence rates and high computational costs. In this work, we introduce an approach that leverages continuous dynamical systems to design a novel denoising network for diffusion models that is more parameter-efficient, exhibits faster convergence, and demonstrates increased noise robustness. Experimenting with denoising probabilistic diffusion models, our framework operates with approximately a quarter of the parameters and $\sim 30\%$ of the Floating Point Operations (FLOPs) compared to standard U-Nets in Denoising Diffusion Probabilistic Models (DDPMs). Furthermore, our model is faster in inference than the baseline models when measured in equal conditions while converging to better quality solutions.

1 Introduction

Diffusion Probabilistic Models (DPMs), stemming from the work of [1] and expanded by others (e.g. [2], [3]), have excelled in domains like image, audio, and video synthesis using an iterative sampling mechanism. However, generating top-tier samples often demands a significant number of iterations, with the diffusion models requiring up to 2000 times more computational power compared to other generative models ([4], [5], [6]). While recent attempts to boost DPMs' efficiency have emerged, like early stopping [7] or modified sampling [8] among others (e.g. [9], [10], [11], [12], [13]), however, they do not improve on parameter and operational efficiency.

In this paper, we redefine the reverse process in diffusion models by enhancing the denoising network architecture. Current research mainly uses U-Net architectures for discrete denoising, including notable frameworks like Stable Diffusion [14]. Many limitations arise from the network's inherent constraints. Inspired by the works of that [15, 16], we employ deep implicit layers to devise a superior denoising network that is more efficient, converges swiftly, and outperforms traditional U-Nets. We show that our architectural shift also directly improves inference time. Importantly, our method is orthogonal to existing performance enhancement techniques, allowing their integration for further advances. In particular, our contributions are:

- We propose a new denoising network that incorporates an original dynamic Neural ODE block integrating residual connections and time embeddings for the temporal adaptivity required by diffusion models.
- We develop a novel family of diffusion models that uses a deep implicit U-Net denoising network; as an alternative to the standard discrete U-Net. This approach improves efficiency, robustness, and noise reduction.
- We evaluate our framework, demonstrating competitive performance in image synthesis with 4x fewer parameters, lower memory, and faster inference under equal conditions.

*University of Oxford, UK <sergio.calvoordonez@maths.ox.ac.uk>; †Imperial College London, UK; ‡University of Cambridge, UK.

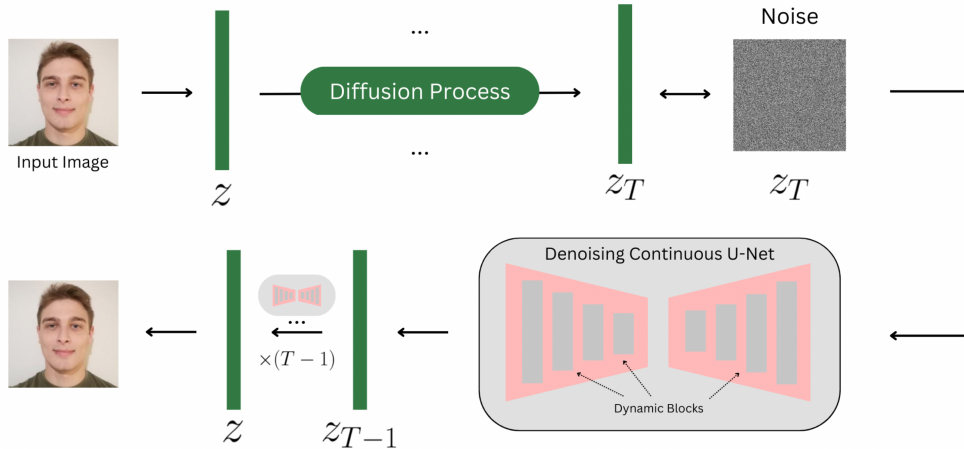


Figure 1: Visual representation of our framework featuring implicit deep layers tailored for denoising in the reverse process of a diffusion model, enabling the reconstruction of the original data from a noise-corrupted version.

2 Methodology

In standard DDPMs, the reverse process involves reconstructing the original data from noisy observations through a series of discrete steps using variants of U-Net architectures. In contrast, our approach (Fig. 1) employs a continuous U-Net-inspired (cU-Net) solution to model the reverse process in a *locally continuous-time setting*¹.

Unlike previous work on continuous U-Nets, focusing on segmentation [16], we rethink the architecture for denoising in diffusion models. We adjusted the output channels for image channel equivalence, and the loss function transitioned from a categorical cross-entropy loss to a reconstruction-based loss that measures pixel discrepancies between the denoised image and the original. The importance of preserving spatial resolution in denoising tasks led to adjusting stride values in the continuous U-Net for reduced spatial resolution loss, with the dynamic blocks being optimised for enhanced noise management. Importantly, time embeddings are introduced to the network, facilitating the accurate modelling of the diffusion process across time steps, enabling the continuous U-Net to adapt dynamically to specific diffusion stages. Therefore, our continuous U-Net model’s architecture is tailored to capture the dynamics in the diffusion model and includes features like residual connections and attention mechanisms to understand long-range data dependencies.

2.1 Dynamic Blocks for Diffusion Models

Our design incorporates a neural network function approximator block (Fig. 2 - right), representing the derivative in the ODE form $\frac{dz}{dt} = f(t, z)$ which dictates how the hidden state z evolves over the continuous-time variable t . Group normalisation layers are employed for feature scaling, followed by convolutional operations for spatial feature extraction. To adapt to diffusion models, we integrate time embeddings using multi-layer perceptrons that adjust the convolutional outputs via scaling and shifting and are complemented by our custom residual connections. Additionally, we use an ODE block (Fig. 2 - left) that captures continuous-time dynamics, wherein the evolutionary path of the data is defined by an ODE function and initial conditions derived from preceding blocks.

2.2 A New ‘U’ for Diffusion Models

As we fundamentally modify the denoising network used in the reverse process, it is relevant to look into how the mathematical formulation of the reverse process of DDPMs changes. The goal is to approximate the transition probability using our model. Denote the output of our continuous U-Net

¹Denotes a hybrid method where, despite an overall discretised framework, each step uses continuous-time modelling for the image’s latent representation, guided by a neural ODE’s dynamics.

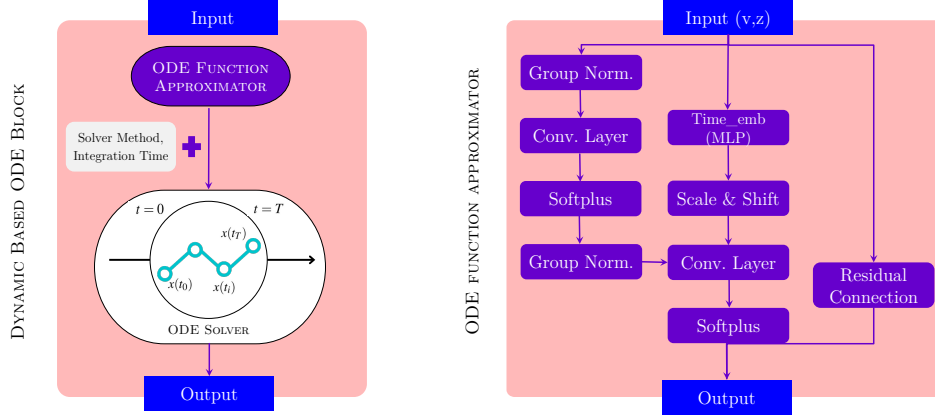


Figure 2: Our modified foundational blocks built into our continuous U-Net architecture. ODE Block (left) and the ODE derivative function approximator (right).

as $\tilde{U}(x_t, t, \tilde{t}; \Psi)$, where x_t is the input, t is the time variable related to the DDPMs, \tilde{t} is the time variable related to neural ODEs and Ψ represents the parameters of the network including θ_f from the dynamic blocks built into the architecture. We use the new continuous U-Net while keeping the same sampling process [3] which reads

$$x_{t-1} = \frac{1}{\sqrt{\alpha_t}} \left(x_t - \sqrt{\beta_t} \frac{1}{\sqrt{1 - \bar{\alpha}_t}} \epsilon_\theta(x_t, t) \right) + \sigma_t z, \text{ where } z \sim \mathcal{N}(0, I) \quad (1)$$

As opposed to traditional discrete U-Net models, this reformulation enables modelling the transition probability using the continuous-time dynamics encapsulated in our architecture. Going further, we can represent the continuous U-Net function in terms of dynamical blocks given by:

$$\epsilon_\theta(x_t, t) \approx \tilde{U}(x_t, t, \tilde{t}; \theta) \quad (2)$$

where,

$$\begin{cases} x''_{\tilde{t}} = f^{(a)}(x_{\tilde{t}}, x'_{\tilde{t}}, t, \tilde{t}, \theta_f) \\ x_{\tilde{t}_0} = X_0, \quad x'_{\tilde{t}_0} = g(x_{\tilde{t}_0}, \theta_g) \end{cases} \quad (3)$$

Here, $x''_{\tilde{t}}$ represents the second-order derivative of the state with respect to time (acceleration), $f^{(a)}(\cdot, \cdot, \cdot, \cdot, \theta_f)$ is the neural network parameterising the acceleration and dynamics of the system, and $x_{\tilde{t}_0}$ and $x'_{\tilde{t}_0}$ are the initial state and velocity. Then we can update the iteration by x_t to x_{t-1} by the continuous network.

3 Experimental Results

We evaluated our method’s efficacy via generated sample quality (Fig. 3). As a baseline, we used a DDPM that uses the same U-Net described in [3]. Samples were randomly chosen from both the baseline DDPM and our model, adjusting sampling timesteps across datasets to form synthetic sets. By examining the FID (Fréchet distance) measure as a timestep function on these datasets, we determined optimal sampling times. Our model consistently reached optimal FID scores in fewer timesteps than the U-Net-based model (Table 1), indicating faster convergence by our continuous U-Net-based approach.

We examined the average inference time per sample across various datasets (Table 1). While both models register similar FID scores, our cU-Net infers notably quicker, being about 30% to 80% faster². Notably, this enhanced speed and synthesis capability is achieved with marked parameter

²Note that inference times reported were measured on a CPU, as current Python ODE-solver packages do not utilize GPU resources effectively, unlike the highly optimised code of conventional U-Net convolutional layers.

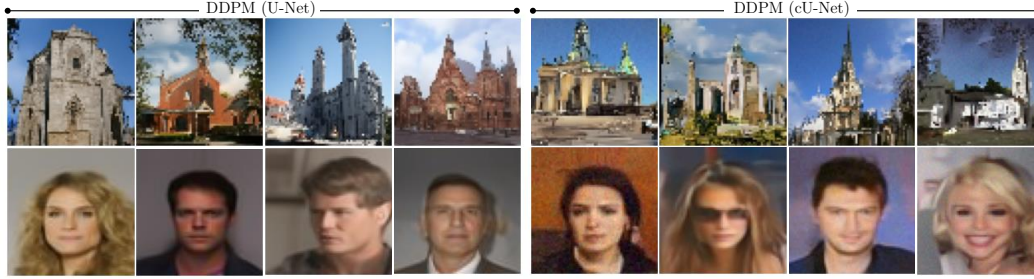


Figure 3: Randomly selected generated samples by our model (right) and the baseline U-Net-based DDPM (left) trained on CelebA and LSUN Church.

BACKBONE	MNIST			CELEBA			LSUN CHURCH		
	FID	Steps	Time (s)	FID	Steps	Time (s)	FID	Steps	Time (s)
U-Net	3.61	30	3.56	19.75	100	12.48	12.28	100	12.14
cU-Net	2.98	5	0.54	21.44	80	7.36	12.14	90	8.33

Table 1: Performance metrics across datasets: FID scores, sampling timesteps (Steps), and average generation time for both the U-Net and continuous U-Net (cU-Net) models.

MODEL	GFLOPS	MB
U-Net	7.21	545.5
Continuous UNet (cU-Net)	2.90	137.9
cU-Net wo/A (no attention)	2.81	128.7
cU-Net wo/R (no resblocks)	1.71	92.0
cU-Net wo/A/R (no attention & no resblocks)	1.62	88.4

Table 2: Number of GigaFLOPS (GFLOPS) and Megabytes in Memory (MB) for Different Models.

efficiency. As seen in Fig. 4, our model (yellow) uses roughly a quarter of the parameters compared to the baseline DDPM (red).

We further demonstrate our architecture’s computational efficiency through FLOPS and memory storage metrics. Table 2 indicates our model improves upon the baseline in terms of FLOPS and uses just 25% of the memory storage compared to the standard U-Net in DDPMs across the literature. Fig. 4 and Table 2 show measurements of our model without key components, such as attention mechanisms and residual connections, emphasising that our efficiency primarily stems from the architectural design, not just component interaction.

4 Conclusion

We explored the scalability of continuous U-Net architectures, introducing attention mechanisms, residual connections, and time embeddings tailored for diffusion timesteps. Our innovations offer notable efficiency advantages over traditional diffusion models, reducing computational demands and hinting at possible deployment on resource-limited devices due to their parameter efficiency while providing comparable synthesis performance. Considerations for future work go around improving the ODE solver parallelisation and incorporating sampling techniques to further boost efficiency.

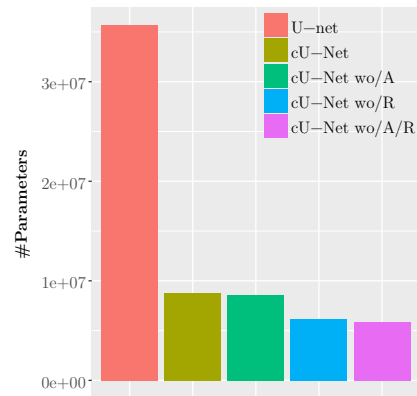


Figure 4: Total number of parameters for U-Net and continuous U-Net (cU-Net) models and variants. Notation follows Table 2.

Acknowledgments

SCO gratefully acknowledges the financial support of the Oxford-Man Institute of Quantitative Finance. A significant portion of SCO’s work was conducted at the University of Cambridge, where he also wishes to thank the University’s HPC services for providing essential computational resources. AAR gratefully acknowledges funding from the Cambridge Centre for Data-Driven Discovery and Accelerate Programme for Scientific Discovery, made possible by a donation from Schmidt Futures, ESPRC Digital Core Capability Award, and CMIH and CCIMI, University of Cambridge.

References

- [1] Jascha Sohl-Dickstein, Eric Weiss, Niru Maheswaranathan, and Surya Ganguli. Deep unsupervised learning using nonequilibrium thermodynamics. In *International conference on machine learning*, pages 2256–2265. PMLR, 2015.
- [2] Yang Song, Jascha Sohl-Dickstein, Diederik P Kingma, Abhishek Kumar, Stefano Ermon, and Ben Poole. Score-based generative modeling through stochastic differential equations. *arXiv preprint arXiv:2011.13456*, 2020.
- [3] Jonathan Ho, Ajay Jain, and Pieter Abbeel. Denoising diffusion probabilistic models. *Advances in neural information processing systems*, 33:6840–6851, 2020.
- [4] Yang Song and Stefano Ermon. Generative modeling by estimating gradients of the data distribution. In *Neural Information Processing Systems*, 2019.
- [5] Ian Goodfellow, Jean Pouget-Abadie, Mehdi Mirza, Bing Xu, David Warde-Farley, Sherjil Ozair, Aaron Courville, and Yoshua Bengio. Generative adversarial networks. *Communications of the ACM*, 63(11):139–144, 2020.
- [6] Danilo Rezende and Shakir Mohamed. Variational inference with normalizing flows. In *International conference on machine learning*, pages 1530–1538. PMLR, 2015.
- [7] Zhaoyang Lyu, Xudong Xu, Ceyuan Yang, Dahua Lin, and Bo Dai. Accelerating diffusion models via early stop of the diffusion process. *arXiv preprint arXiv:2205.12524*, 2022.
- [8] Jiaming Song, Chenlin Meng, and Stefano Ermon. Denoising diffusion implicit models. *arXiv preprint arXiv:2010.02502*, 2020.
- [9] Fan Bao, Chongxuan Li, Jun Zhu, and Bo Zhang. Analytic-dpm: an analytic estimate of the optimal reverse variance in diffusion probabilistic models. *arXiv preprint arXiv:2201.06503*, 2022.
- [10] Hyungjin Chung, Byeongsu Sim, Dohoon Ryu, and Jong Chul Ye. Improving diffusion models for inverse problems using manifold constraints. *Advances in Neural Information Processing Systems*, 35:25683–25696, 2022.
- [11] Alexander Quinn Nichol and Prafulla Dhariwal. Improved denoising diffusion probabilistic models. In *International Conference on Machine Learning*, pages 8162–8171. PMLR, 2021.
- [12] Konpat Preechakul, Nattanat Chatthee, Suttisak Wizadwongsa, and Supasorn Suwajanakorn. Diffusion autoencoders: Toward a meaningful and decodable representation. In *Proceedings of the IEEE/CVF Conference on Computer Vision and Pattern Recognition*, pages 10619–10629, 2022.
- [13] Tim Salimans and Jonathan Ho. Progressive distillation for fast sampling of diffusion models. *arXiv preprint arXiv:2202.00512*, 2022.
- [14] Robin Rombach, Andreas Blattmann, Dominik Lorenz, Patrick Esser, and Björn Ommer. High-resolution image synthesis with latent diffusion models. In *Proceedings of the IEEE/CVF conference on computer vision and pattern recognition*, pages 10684–10695, 2022.
- [15] Ricky TQ Chen, Yulia Rubanova, Jesse Bettencourt, and David K Duvenaud. Neural ordinary differential equations. *Advances in neural information processing systems*, 31, 2018.
- [16] Chun-Wun Cheng, Christina Runkel, Lihao Liu, Raymond H Chan, Carola-Bibiane Schönlieb, and Angelica I Aviles-Rivero. Continuous u-net: Faster, greater and noiseless. *arXiv preprint arXiv:2302.00626*, 2023.